

Photonic properties of bicontinuous cubic microphases

M. Maldovan, A. M. Urbas, N. Yufa, W. C. Carter, and E. L. Thomas*

Department of Materials Science and Engineering, Massachusetts Institute of Technology, Cambridge, Massachusetts 02139

(Received 14 November 2001; published 16 April 2002)

Band structures of three dimensionally periodic bi- and tricontinuous cubic structures have been calculated using the plane-wave method for solving Maxwell's equations. In particular, we consider the single primitive, single diamond, single gyroid, double primitive, double gyroid, and double diamond level surface families as examples of such structures found in self-organizing systems. We also provide design guidelines for creating three-dimensional photonic crystals with a complete photonic band gap from block copolymer systems and other self-organizing systems.

DOI: 10.1103/PhysRevB.65.165123

PACS number(s): 42.70.Qs

I. INTRODUCTION

Self-assembly is emerging as a viable technology for the formation of large scale photonic materials. The pattern forming capabilities of self-organizing systems have been extensively explored for a wide variety of applications requiring nanoscale structures. More recently photonic crystals have been formed from self-organizing system such as colloids and block copolymers (BCPs).¹ BPs promise simple, nonlithographic routes to complex morphologies that have interesting and important photonic properties.

Block copolymers belong to a class of self-organizing materials including amphiphiles and surfactants which form a wide range of microstructures.² These microstructures are at times one, two, or three dimensionally periodic and may be discrete or continuous.³ These phases are separated by a sharp interface known as the intermaterial dividing surface (IMDS). Among the most interesting microdomain structures are the single primitive (SP), single diamond (SD), single gyroid (SG), double primitive (DP), double diamond (DD), and double gyroid (DG) that form two or three independent but interconnected domains (one or two networks and a matrix) of cubic symmetry.

Since the networks and matrix are both three dimensionally periodic and continuous, if one type of domain is extracted via etching, for example, and the other component was a rigid material, the structure would be free standing. The three-dimensional (3D) continuity also provides access throughout the bulk of the material for reagents, etchants, and fillers, which affords their use as material templates. Controlled dielectric contrast can be achieved in such photonic materials by etching and/or back filling. These properties make these structures very desirable for large three-dimensional photonic devices.

It has been shown that the IMDS of the SP-, SD-, SG-, DP-, DD-, and DG-type morphologies in actual materials can be approximated by surfaces of constant mean curvature (CMC).⁴ These CMC surfaces cannot be exactly represented with an analytical expression but for this set of CMC families there corresponds an approximate level set surface family.⁵ A level set is surface derived from a characteristic equation and a variable parameter. Each unique equation specifies a level set surface family. Level set surface families are identified by their symmetry group. Each structure is as-

sociated with a symmetry group identifier from the International Tables of Crystallography as follows; the single primitive (SP) $Pm3m$, double primitive (DP) $Im3m$, single gyroid (SG) $I4_132$, double gyroid (DG) $Ia3d$, single diamond (SD) $Fd3m$, and double diamond (DD) $Pn3m$. The single level surface families divide space into two regions. The form of the surface is controlled by an analytical expression that is characteristic of the family and the parameter t , which determines the volume fraction of the two regions. For $t=0$ each level surface family approximates the constant mean curvature minimal surface, primitive (P), diamond (D), or gyroid (G), respectively. The minimal surface is a unique member of the family, and is characterized by zero mean curvature and division of space in halves. Double level set surface families are characterized by a different but related analytical expression and two parameters, s and t . These structures divide space into three regions; two networks that interpenetrate but do not connect, and a matrix.

Members of each of these families have been observed in self-assembling systems. The double gyroid structure is known to exist in a variety of A/B diblock and triblock copolymers^{6,7} as well as ABC terpolymer systems⁸ for a particular range of compositions. The DG structure also occurs in certain block copolymer/block copolymer and block copolymer/homopolymer blend systems.⁹ The DP structure has recently been documented in a polymer/ceramic precursor composite¹⁰ which, when calcined, yields a ceramic/air structure with the same morphology. The DD morphology has been observed in a miktoarm star copolymer system of styrene and isoprene.¹¹ In addition, ABC terpolymer materials exhibiting a DG morphology have generated structures where the A and C blocks form networks that are chemically distinct.⁸ Etching one of the networks (by selectively attacking a single block, for example) would yield an SG template. It remains to be seen whether the DP and DD morphologies as well can be accessed with ABC terpolymers.

In order to use these materials in photonic applications, we must understand how to design the system for maximum performance. This is most effectively accomplished by mapping the photonic band structures of these morphologies over a range of materials parameters and structural characteristics. From these photonic property or photonic "gap" maps we can extract the necessary information for constructing a materials system which will form, via self-assembly, a three-

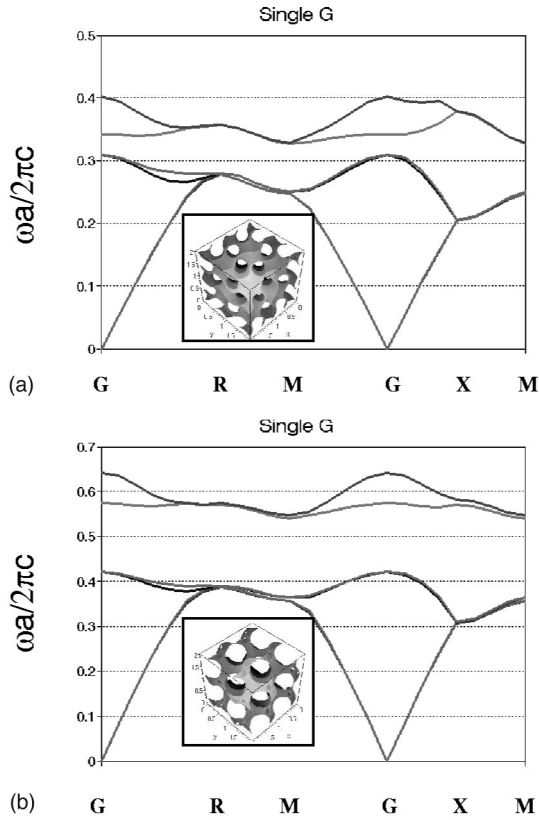


FIG. 1. First six bands for the single G structure. The dielectric contrast is given by $\epsilon_1=1.0$, $\epsilon_2=13.0$. (a) $t=0.0$ (volume fraction=0.5), (b) $t=-1.0$ (volume fraction=0.17).

dimensional photonic crystal with a full band gap for a desired frequency range. This will bring self-assembled photonic devices one step closer to realization.

II. BAND-GAP CALCULATIONS

The propagation of the electromagnetic waves is studied in periodic dielectric structures by numerically solving Maxwell's equations. The plane-wave method is used in the full vectorial formulation.¹²⁻¹⁴ The photonic structure is characterized by the real dielectric constant $\epsilon(\mathbf{r})$. The magnetic permeability $\mu(\mathbf{r})$ is considered constant and equal to 1 throughout the structure. By combining the Maxwell equations with the fundamental equation for the electric field \mathbf{E} is obtained:

$$\nabla \times \nabla \times \mathbf{E} = \frac{\omega^2}{c^2} \epsilon(\mathbf{r}) \mathbf{E},$$

where ω is the angular frequency and c is the speed of light.

The dielectric constant and the electric field are expanded in a sum of plane waves and substituted into the fundamental equation. The following generalized eigenvalue problem is obtained:

$$(\mathbf{k} + \mathbf{G}) \times [(\mathbf{k} + \mathbf{G}) \times \mathbf{E}(\mathbf{G})] + \frac{\omega^2}{c^2} \sum_{\mathbf{G}'} \epsilon(\mathbf{G} - \mathbf{G}') \times \mathbf{E}(\mathbf{G}') = 0,$$

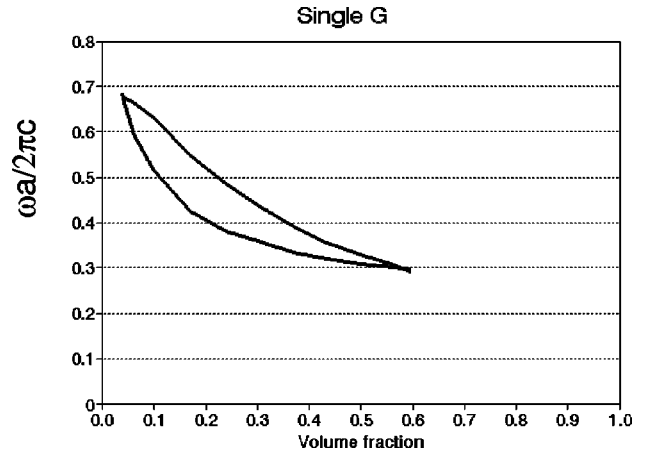


FIG. 2. Gap map of SG structure with 13:1 dielectric contrast. The maximum gap occurs for a volume fraction of 17% dielectric network. This is within the range of the volume fraction of a single network for a block copolymer exhibiting the double gyroid phase.

where \mathbf{k} is the wave vector and \mathbf{G} are the reciprocal-lattice vectors.

As a consequence of considering real dielectric constants (zero loss media) both matrixes are Hermitian. The eigenvalue matrix equation is solved by using LAPACK subroutines

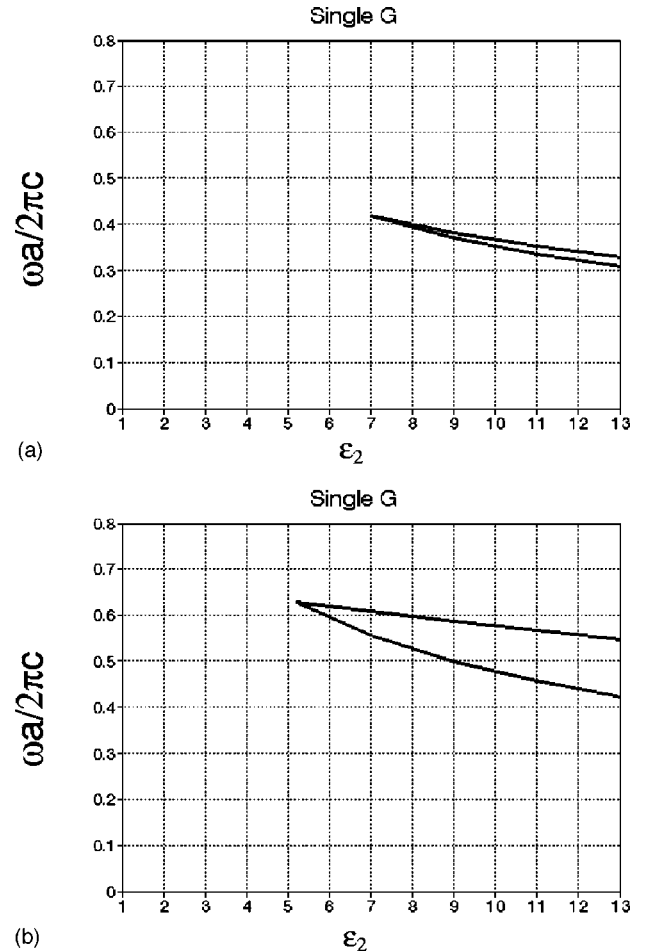


FIG. 3. (a) 50% volume fraction, (b) 17% volume fraction.

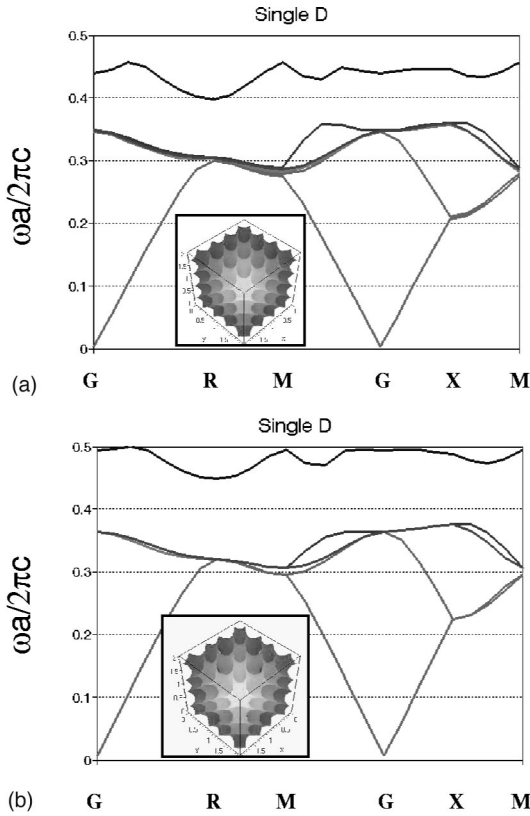


FIG. 4. First six bands for the single D structure at a dielectric contrast of 13:1. (a) $t = 0.0$ (volume fraction = 0.5), (b) $t = -0.2$ (volume fraction = 0.42).

to obtain the propagating frequencies for the corresponding values of the wave vector \mathbf{k} . We use 2187 plane waves to obtain the results. This gives an accuracy of better than 2% in the lower-lying eigenvalues.

Band structures were calculated for the SP, SD, SG, DP, DD, and DG level surface families. These calculations were made on level set structures and specifying that one side of the surface was composed of a material of dielectric constant ϵ_1 and the other side ϵ_2 . In the case of the double structures,

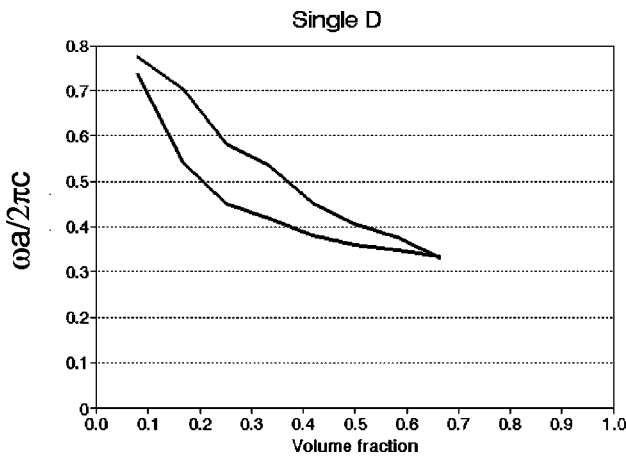


FIG. 5. Gap map of SD structure with 13:1 dielectric contrast. The maximum gap occurs for a volume fraction of 17% dielectric network.

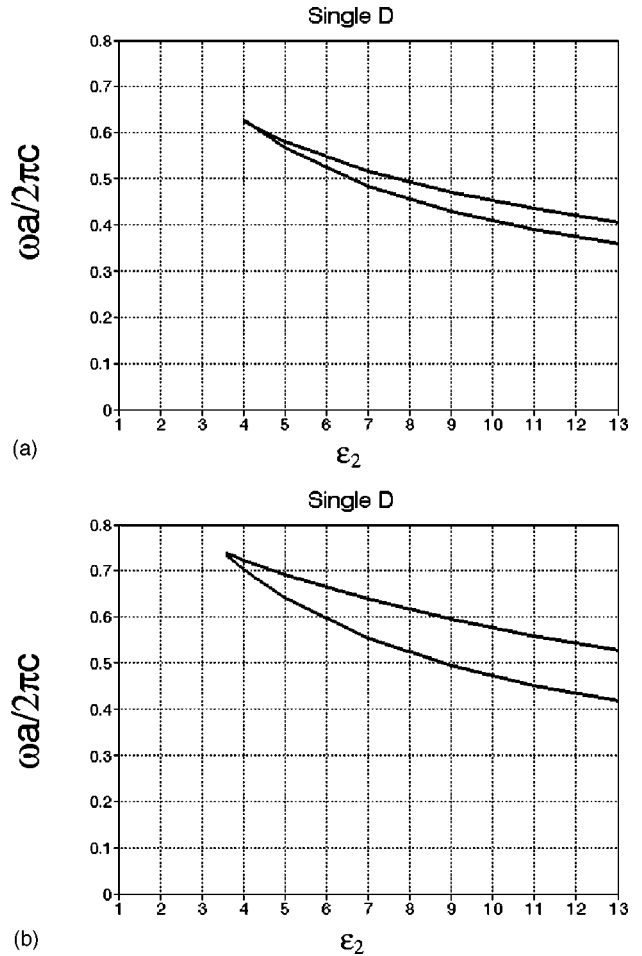


FIG. 6. (a) 50% volume fraction, (b) 34% volume fraction.

both networks have the same dielectric constant. In general, the lower dielectric material was assumed to be air with $\epsilon_1 = 1$ and the higher dielectric material was varied over the range ($\epsilon_2 = 1 - 20$) to examine the dependence of the photonic properties on the dielectric contrast, or ratio of dielectric constants.

The model surfaces were calculated based on formulas derived from families of level sets.⁵ Choosing $t = 0$, approximates the P, D, and G minimal surfaces ($H = 0$). P, D, and G are associate surfaces and evenly divide space between the sides of the surface. The band structures of the exact minimal surfaces P, D, and G were first computed by Martin-Moreno *et al.*¹⁵ using finite difference time domain (FDTD) analysis. (Band diagrams calculated using the plane-wave method on our approximate minimal surfaces were in close agreement with these published results). The t parameter determines the volume fraction occupied by each component of the structure, the network(s) and matrix. Varying t allows exploration of the compositional dependence of the photonic properties and also permits assessment of experimentally realized block polymer structures.

III. RESULTS

Calculated band diagrams of a representative example of each level surface family and a 3D rendering of the surface

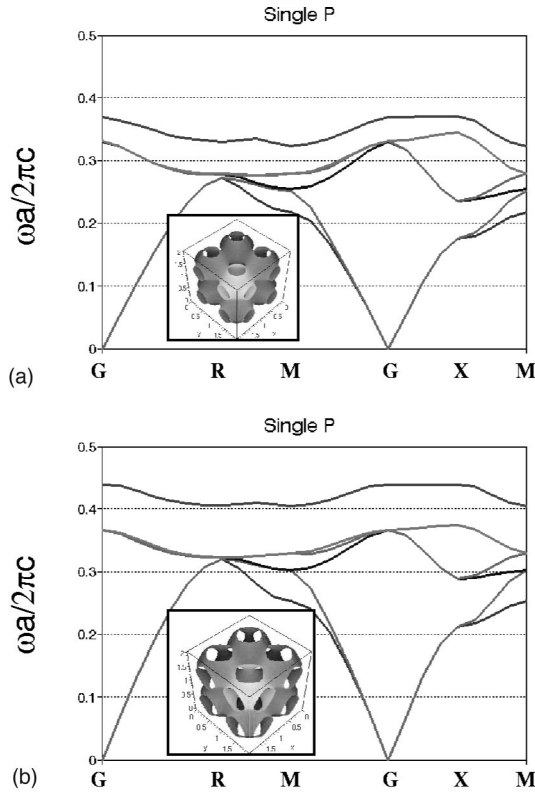


FIG. 7. First six bands for the single P structure at a dielectric contrast of 13:1. (a) $t=0.0$ (volume fraction=0.5), (b) $t=-0.6$ (volume fraction=0.33).

are presented in Figs. 1–3 (Ref. 16). The rendering in each figure is at the volume fraction appropriate for that figure. The surface shown is derived from that used in the calculation. An important feature of these band diagrams is the presence or absence of a complete gap in the frequency domain between the lower set of bands and the upper. Complete gaps are highlighted in yellow for the SG, SD, and SP surface structures. The DG, DD, and DP structures show no evidence of a complete gap at any volume fraction for the range of dielectric contrast [$\epsilon = 1-20$] and normalized frequency explored. For the SG structure, the parameter t was varied within the range ± 1.4 . Band diagrams for $t=0.0$ and $t=-1.0$ are shown in Figs. 1(a) and (b) where the dielectric contrast between the dielectric media is 13:1. For the 50-vol-% structure, a complete gap is found in the range 0.309–0.327 ($\Delta\omega/\omega_0=0.057$). However, the results show that a significantly wider complete gap over the frequencies range 0.421–0.540 ($\Delta\omega/\omega_0=0.247$) can be found for dielectric network volume fraction of 17%.

By varying the parameter t , one can map out the range over which a complete gap exists. The width of the gap with respect to volume fraction is displayed in Fig. 2. The calculations show that the SG structure exhibits a complete gap for volume fractions from 0.04 to 0.60. The maximum value is reached approximately for a volume fraction of 0.17.

If the dielectric contrast between the media is decreased, the gap decreases. Figure 3 shows how the gap varies with dielectric constant for volume fractions of 50% and 17% dielectric network. The dielectric values of medium 2 for

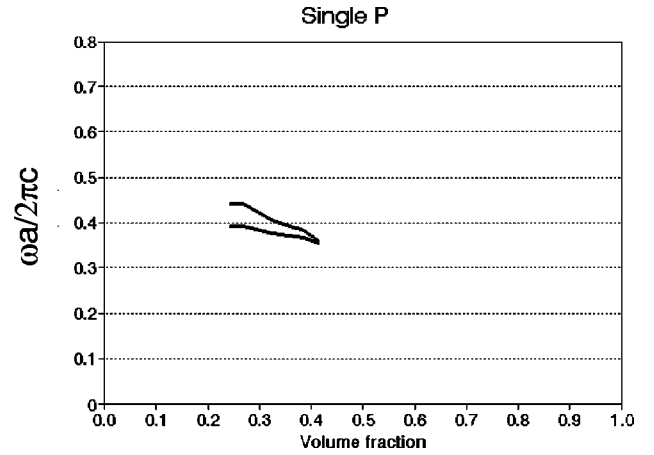


FIG. 8. Gap map of SP structure with 13:1 dielectric contrast. The gap is not shown closing at low volume fractions because lack of computational accuracy prevents assigning bounds to the gap.

which the gap closes are $\epsilon_2 \approx 7$ at 50% and $\epsilon_2 \approx 5.2$ at 17% volume fraction of the dielectric network.

The analysis was repeated for the SD structure. In this case the parameter t was varied from -1.2 to 1.2 . The band diagram for $t=0.0$ (50% volume fraction) shown in Fig. 4(a) produces a gap in the range 0.360–0.398 ($\Delta\omega/\omega_0=0.1$), in agreement with Martin-Moreno *et al.*¹⁵ In Fig. 4(b) the band structure for $t=-0.2$ (42% volume fraction) is presented showing a gap 0.376–0.448 ($\Delta\omega/\omega_0=0.175$).

Figure 5 shows the variation of the complete gap with volume fraction for SD. A complete gap is found for volume fractions between 0.08 and 0.66 and is largest for a volume fraction of 0.17. The closing of the gap via decrease of the dielectric constant for the SD was also studied. The results obtained for 50 and 34% network volume fraction are shown in Figs. 6(a) and (b), respectively. It can be observed that a minimum dielectric contrast of 3.6 is needed to obtain a complete gap for 34% volume fraction.

Figures 7(a) and (b) show the corresponding analysis for SP. In agreement with Martin-Moreno *et al.*,¹⁵ Fig. 7(a) shows the absence of a complete gap at 50% network volume fraction. A gap opens for small dielectric network volume fractions. As a consequence, the accuracy is lower for these calculations. Figure 7(b) shows a gap in the range 0.374–0.404 ($\Delta\omega/\omega_0=0.077$) for 0.33 network volume fraction (see Fig. 8).

For the SP structure the closing of the gap was studied for 0.33 network volume fraction. The results obtained show that the minimum contrast of 8.5 needed to have a complete gap is much higher than that for the SD or SG structures (see Fig. 9).

Finally, the double structures, DG, DD, and DP, were studied. None of these show gaps for the range of parameters analyzed. For the DG case, a pseudogap can be found in particular cases (Fig. 10).

IV. CONCLUSIONS

We have shown that six families of connected three-dimensional morphologies exhibiting various types of cubic

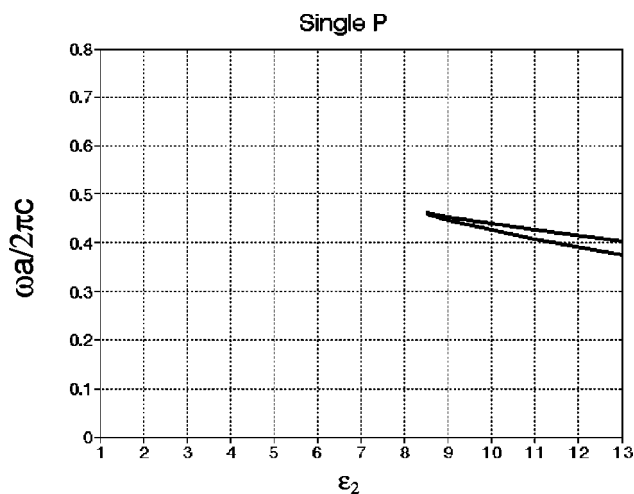


FIG. 9. Single P at 33% volume fraction where it achieves a complete band gap for the lowest dielectric contrast.

symmetry possesses a wide range of parameters for which complete photonic gaps exist for the *single network* members. Interestingly, the double network variants possess no complete gaps for the parameter space studied. This shows that the increase in symmetry of the multiregion system destroys this property of the system. Design guidelines for obtaining robust photonic band gaps in the SD, SP, and DP morphologies have been given in the form of gap maps for a range of volume fractions and dielectric contrasts. The SD network (space group $Fd3m$) at a network volume fraction of 34% exhibits a complete band gap at a dielectric contrast of 3.6. This value is comparable to the best structures studied to date¹⁷ and is notably lower than dielectric or air spheres arranged on a diamond lattice.¹⁸ The volume fraction, how-

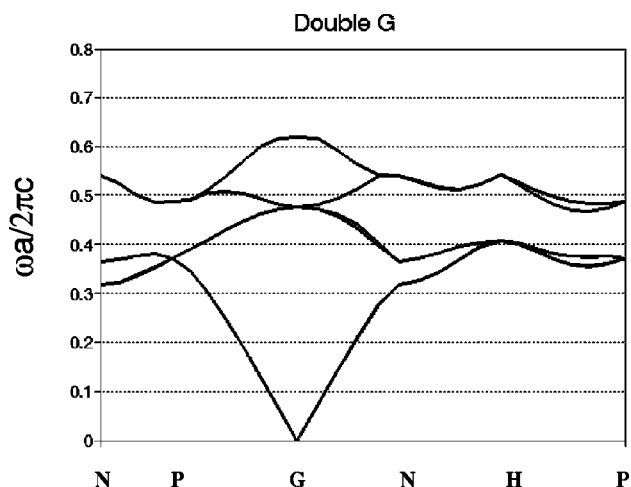


FIG. 10. Double G at 38% volume fraction showing a pseudogap. In this case the density of states goes to unity for a particular frequency.

ever, of dielectric where the gap opens at the lowest index contrast is the same as for dielectric spheres on a diamond lattice. The multiregion systems have been observed in block copolymer based self-organizing materials. The double structures can be tailored such that the two networks become chemically distinct decreasing the symmetry and yielding a possible pathway for forming these single, 3D morphologies at optical length scales.¹⁶ Future work will concentrate on fabrication of the single network ordered systems.

ACKNOWLEDGMENTS

The authors would like to acknowledge NSF, AFOSR, the NSF-supported Center for Materials Science and Engineering, and MIT.

*Corresponding author, Room 13-5094, 77 Massachusetts Ave., Department of Materials Science and Engineering, MIT, Cambridge, MA 02139.

¹A. C. Edrington, A. M. Urbas, P. DeRege, C. X. Chen, T. M. Swager, N. Hadjichristidis, M. Xenidou, L. J. Fetters, J. D. Joannopoulos, Y. Fink, and E. L. Thomas, *Adv. Mater.* **13**, 421 (2001).

²C. Tschierske, *Annu. Rep. Prog. Chem., Sect. C: Phys. Chem.* **97**, 191 (2001).

³E. L. Thomas and R. L. Lescanec, *Philos. Trans. R. Soc. London, Ser. A* **348**, 149 (1994).

⁴E. L. Thomas, D. M. Anderson, C. S. Henkee, and D. Hoffman, *Nature (London)* **334**, 598 (1988).

⁵M. Wohlgenuth, N. Yufa, J. Hoffman, and E. L. Thomas, *Macromolecules* **34**, 6083 (2001).

⁶D. A. Hajduk, P. E. Harper, S. M. Gruner, C. C. Honeker, G. Kim, E. L. Thomas, and L. J. Fetters, *Macromolecules* **27**, 4063 (1994).

⁷A. Avgeropoulos, B. J. Dair, N. Hadjichristidis, and E. L. Thomas, *Macromolecules* **30**, 5634 (1997).

⁸J. Suzuki, M. Seki, and Y. Matsushita, *J. Chem. Phys.* **112**, 4862

(2000).

⁹R. G. H. Lammertink, M. A. Hempenius, E. L. Thomas, and G. J. Vancso, *J. Polym. Sci., Part B: Polym. Phys.* **37**, 1009 (1999).

¹⁰A. C. Finnefrock, R. Ulrich, A. Du Chesne, C. C. Honeker, K. Schumacher, K. K. Unger, S. M. Gruner, and U. Wiesner, *Angew. Chem. Int. Ed. Engl.* **40**, 1207 (2001).

¹¹Y. Tselikas *et al.*, *Macromolecules* **29**, 3390 (1996).

¹²K. M. Leung and Y. F. Liu, *Phys. Rev. Lett.* **65**, 2646 (1990).

¹³Z. Zhang and S. Satpathy, *Phys. Rev. Lett.* **65**, 2650 (1990).

¹⁴H. S. Sözüer and J. W. Haus, *Phys. Rev. B* **45**, 13 962 (1992).

¹⁵L. Martin-Moreno, F. J. Garcia-Vidal, and A. M. Somoza, *Phys. Rev. Lett.* **83**, 73 (1999).

¹⁶The authors direct readers to the website www.msri.org/publications/sgp/SGP/ for further visualizations of the three-dimensional structures discussed in this paper.

¹⁷K. M. Ho, C. T. Chan, and C. M. Soukoulis, *Solid State Commun.* **89**, 413 (1994).

¹⁸K. M. Ho, C. T. Chan, and C. M. Soukoulis, *Phys. Rev. Lett.* **65**, 3152 (1990).